

Received December 25, 2021, accepted January 21, 2022, date of publication January 31, 2022, date of current version February 9, 2022.

Digital Object Identifier 10.1109/ACCESS.2022.3147829

Link Budget Analysis for LEO Satellites Based on the Statistics of the Elevation Angle

JUAN MISAEL GONGORA-TORRES^{ID}, (Graduate Student Member, IEEE),

CESAR VARGAS-ROSALES^{ID}, (Senior Member, IEEE),

ALEJANDRO ARAGÓN-ZAVALA^{ID}, (Senior Member, IEEE),

AND RAFAELA VILLALPANDO-HERNANDEZ^{ID}

School of Engineering and Science, Tecnológico de Monterrey, Monterrey 64849, Mexico

Corresponding author: Juan Misael Gongora-Torres (jmgongora@yandex.com)

ABSTRACT Link budgets are widely applied to evaluate communication links for low Earth Orbit (LEO) satellites. However, approaches to calculate the received power from LEO satellites have followed similar procedures to those for Geostationary (GEO) satellites and other fixed distance wireless systems, ignoring the satellite mobility that causes continuous changes in the path length and in the elevation angle. Link budgets found in the literature for LEO communication systems have commonly opted to characterize the best and worst-cases of the received signal; however, this common approach tells little about how often those cases occur, and little can be inferred about the expected received power and its measures of dispersion. This article introduces an innovative methodology to evaluate LEO link budgets using the long term statistics and probabilities of occurrence of the elevation angle, which is characterized in this work through a random variable. This characterization of the elevation angle through a random variable allows the calculation of the expected value of the received power, its standard deviation, quantiles, among other quantities. The received power is essential to calculate other link indicators such as the carrier-to-noise ratio (C/N), and with the proposed methodology it can be now calculated considering the path length and elevation angle variability that occur for LEO satellites.

INDEX TERMS Elevation angle, LEO, link budget, NGEO, satellite communications.

I. INTRODUCTION

The number of Low Earth Orbit (LEO) satellites has significantly increased since the Iridium constellation deployment in the '90s and now this number increases and represents the potential infrastructure for the next generation satellites planned to be massively deployed, [1]. LEO has been particularly popular for deployment of small satellites such as CubeSats, because there are several advantages for small and big satellites at LEO compared to higher orbits, such as a shorter path length and round trip time (RTT). Nevertheless, there are also more challenges, one of which is the time-varying nature of the channel produced by the mobility of the satellite over the Earth at high speeds.

The LEO satellite channel has not been treated thoroughly in the literature as the geostationary Earth orbit (GEO) channel has. One notorious difference between those two chan-

The associate editor coordinating the review of this manuscript and approving it for publication was Pietro Savazzi^{ID}.

nels is that GEO often considers a fixed elevation angle, θ . However, for LEO, from the early works describing this channel, [2], up to more recent approaches, [3], it has been notorious the need to consider the variations of θ in order to characterize the channel and calculate the received signal power.

The receiver environment modifies the transmitted signal through effects such as multipath and shadow fading; however, models including those effects are only valid for specific locations with similar characteristics. The link budget calculates link quality based on received power, and in general the receiver environment effects are not considered relevant. This has been widely used in the past in satellite and ground wireless communications.

The satellite link budget is thus a calculation of the received power at the spacecraft or Earth station (ES). Discussions and examples about this topic are comprehensively explained in many satellite communications books such as [4] and [5], whereas a brief review about additional

operational considerations is available in [6]. Even though the link budget is usually developed for every satellite mission during the planning stage, as in [7], [8], and [9], little work has been done to adapt it for spacecraft operating at LEO.

Typical link analysis assume independence between the factors that cause attenuation, allowing to calculate the received power as a product of gains, losses, and system performance indicators (such as noise temperature of the receiver, or figure of merit) [10]. A detailed explanation of the factors affecting the link is available in [11]. However, the main challenge for LEO link budgets is not the calculation of the attenuation and atmospheric losses [12], but how to integrate those with the spacecraft mobility over the Earth's surface [13], [14].

Link budgets have been applied for LEO small satellites by many works [15]–[18] in the same way as it has been for GEO, and fixed distance wireless communications using best and worst-cases. For LEO, those cases have been associated with the minimum and maximum value of θ , respectively. Nonetheless, spacecrafts' mobility at LEO make the best and worst-cases provide a minimal description of the link, since those cases do not exhibit the always-occurring path length changes that cause variable received power for the elevation angle values of $\theta_{min} < \theta < \theta_{max}$.

As mentioned previously, traditional satellite link budgets resemble those developed for terrestrial and GEO communication systems, since those contain a best and worst-case scenarios. Nevertheless, from merely those cases it is not possible to determine which one will occur more often. Furthermore, it is not inferable the expected received power, $E[P_R]$, nor are available measures of dispersion such as the standard deviation of P_R , or its quantiles (which come from its cumulative distribution function).

This article presents a link budget analysis for LEO satellites using the long term probabilities of the elevation angle θ . In addition, improvements to the current link budget approach for LEO satellites are achieved, together with better estimations of the received signal power at a particular Earth station (ES) location. The results include basic statistics of the received power, P_R , and allow a description of the link with a probability basis, instead of just using best and worst cases of P_R as it is commonly done for LEO link budgets. The proposed model has been developed for the downlink, however, it can be adapted for the uplink as well. Similarly, the same procedure can be applied for more ES locations and LEO or MEO (medium Earth orbit) configurations.

The structure of the document is as follows, Section II contains the theoretical fundamentals; Section III describes the methodology to calculate the received signal power, and definitions and requirements for the link budget calculations. The results are discussed in Section IV, which contains first a typical LEO link budget analysis, and then one considering the randomness of θ . Finally, Section V contains the conclusions and future work.

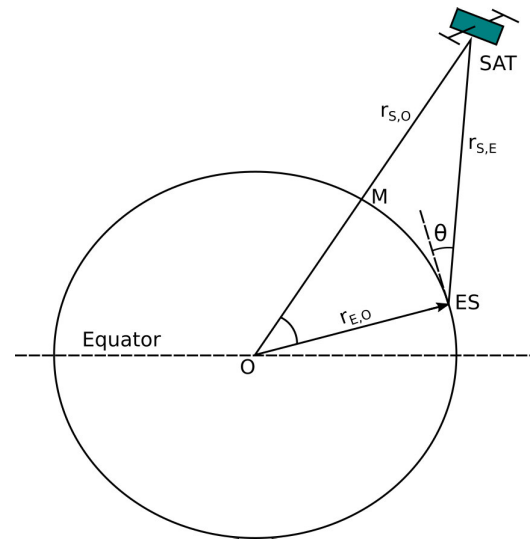


FIGURE 1. Elevation Angle.

II. THEORETICAL FUNDAMENTALS

This section contains the theoretical fundamentals that constitute the base of the link budget analysis proposed. First some important parameters are introduced in order to explain the working scenario. After that, the link budget is defined including its relationship with other link indicators.

A. ELEVATION ANGLE

The angle between the ES and the satellite taking as a reference the local horizon line is known as elevation angle, θ . The calculation of θ is typically derived from the geometric relations of the instantaneous position of a satellite and an ES.

A procedure to calculate θ , as described by [19], is

$$\theta = \arctan \left(\frac{\cos \Delta \cos \phi_{ES} - (r_{E,O}/r_{S,O})}{\sqrt{1 - \cos^2 \Delta \cos^2 \phi_{ES}}} \right), \quad (1)$$

where $r_{E,O}$ and $r_{S,O}$ are the distances from the center of the Earth to the ES and the satellite, respectively; and ϕ_{ES} is the latitude at which the ES is located in degrees. The subsatellite point, M, corresponds to the latitude and longitude of the satellite instantaneous position, and Δ is the difference in longitude between the ES and M in degrees. Fig.1 contains a graphical description of θ , where the center of the Earth is labeled as O . Table 1 contains a selected group of abbreviations to facilitate reading through the different sections of the document.

B. OUTAGE PROBABILITY

The outage probability, P_{out} , describes the proportion of time that the link is unavailable and it is often expressed as the probability of the received signal power in dBW, P_R , being below a power threshold, P_{th} , that is

$$P_{out} = P(P_R \leq P_{th}). \quad (2)$$

In satellite communications, P_{out} depends on several conditions such as the distance between the satellite and the ES, $r_{S,E}$, the atmospheric attenuation, A_{Atm} , and interference from ground and space sources, I . The total attenuation in dB's, A_T , is the sum in logarithmic units of A_{Atm} and the free space path loss, L_{FS} .

Assuming negligible depointing losses, interference, and receiver environment effects such as multipath and shadow fading, one can see that P_{out} depends only on the transmitter effective isotropic radiated power (EIRP), the figure of merit, G/T (the ratio of the gain at the receiver antenna, G_R , to the system temperature noise, T_S), and A_T . If it is further assumed that the receiver and transmitter maintain constant their EIRP and G/T values for a contact duration, then, the following equivalence occurs because in this case, A_T is the only cause of outage

$$P(P_R \leq P_{th}) \iff P(A_T \geq A_{th}) \quad (3)$$

where A_{th} is a threshold level of A_T .

For LEO, $r_{S,E}$, A_T , and I depend on the elevation angle, which changes as the satellite moves. As the angle θ decreases, $r_{S,E}$ increases as follows

$$\theta \rightarrow \min(\theta) \iff r_{S,E} \rightarrow \max(r_{S,E}), \quad (4)$$

and similarly

$$\theta \rightarrow \max(\theta) \iff r_{S,E} \rightarrow \min(r_{S,E}), \quad (5)$$

where $\max(r_{S,E})$ occurs at $\theta \leq 90^\circ$ (subject to $\theta > \min(\theta)$) and $\min(r_{S,E})$ at some small value of $\theta \geq 0^\circ$.

A larger distance $r_{S,E}$ causes a higher value of L_{FS} ; however, the same path length dependence of A_{Atm} requires the assumption of the same atmospheric conditions for the shortest and largest paths. Once assumed equal atmospheric conditions A_{Atm} increases for low values of θ , since the atmospheric path becomes larger for lower values of θ . On the other hand, when θ takes values close to 90° , $r_{S,E}$ will be at its minimum, and so does A_T .

Once it is assumed that A_{Atm} and A_T are distance-dependent, from (4) and (5) that dependence can be rewritten in terms of θ as

$$P(A_T \geq A_{th}) \iff P(\Theta \leq \theta_{min}), \quad (6)$$

where Θ is a random variable (to be specified in Section III-A) that takes values of θ , and θ_{min} is the minimum value of θ for which the link is available. Combining (3) and (6), we can relate the outage probability P_{out} through the equivalence of the distribution of the received power to that of the elevation angle

$$P(P_R \leq P_{th}) \iff P(\Theta \leq \theta_{min}). \quad (7)$$

A similar approach to the one developed in (6) and (7) is found in [20] to evaluate the rain attenuation for satellite communications with variable elevation angle θ .

C. THE LINK BUDGET

The link budget calculation is one common method to evaluate the performance of a satellite link. For GEO, $r_{S,E}$ and θ are constant for a large region or typically slowly varying for mobile users traveling at ground speeds; then, its link budget can be evaluated at a fixed distance and constant θ . Additionally, a few propagation cases can describe a GEO link; for example, a two-case model, where the best case is a clear sky, and the worst case when it rains. However, $r_{S,E}$ and θ are always varying between a fixed ES and a LEO satellite.

The link budget equation is commonly defined for GEO and LEO as

$$P_R = P_T + G_T - A_T + G_R, \quad (8)$$

where P_T is the transmitted power, G_T is the transmitter antenna gain, A_T is the total attenuation, and G_R is the receiver antenna gain, and all quantities are in dB's. The received power in dBW, P_R , can be later employed to calculate the carrier-to-noise ratio (C/N), carrier-to-noise plus interference ratio ($C/(N+I)$), carrier-to-noise density ratio (C/N_0), and bit energy-to-noise density ratio (E_b/N_0), by considering the characteristics of the receiver such as system temperature, T_S , modulation, bit rate, and interference.

The methodology to evaluate C/N , C/N_0 , and E_b/N_0 is based on the value of P_R , and the particular system characteristics and requirements. Detailed procedures and examples of those calculations are commonly found in satellite literature such as [1] and [15]. The calculation of $C/(N+I)$ is highly relevant for LEO and discussed in several sources such as [21] and [22]. Examples of strategies to avoid high levels of interference with other satellites are presented in [23].

The definition of θ , derivation of P_R , and link budget description, are employed in the following sections to calculate P_R and its statistics using the elevation angle. However, as previously mentioned, the analysis can be easily extended to compute other link indicators such as C/N_0 , (E_b/N_0) , and $C/(N+I)$.

III. METHODOLOGY

Simulations of a LEO satellite were performed with the parameters shown in Table 2, three remaining orbital parameters, not included in the table, are the argument of perigee, ω , right ascension of the ascending node, Ω , and true anomaly, v ; all of those were set to zero in their initial value. This was considered because these remaining orbital parameters do not affect the statistical behavior of the elevation angle. The initial orbit eccentricity, e , and the inclination, i , were selected with values close to those of real satellites. However, the semi-major axis, a , was only simulated for 1.75 years and for altitudes between 1000 km and 2000 km, since no propulsion system was considered in the simulations and lower altitudes caused more significant orbit perturbations in the selected period. The simulation results included the satellite position, velocity, and contact duration for $\theta \geq 10^\circ$. From the satellite position, parameters $r_{S,E}$ and θ were calculated and recorded with a time step of five seconds.

TABLE 1. Abbreviations.

Abbreviation	Description	Defined in Section
θ	Elevation angle	I
θ_{min}	Minimum elevation angle required to communicate with the satellite	II.B
θ_{max}	Maximum elevation angle that is possible to observe from the ES	III.B
θ'	Auxiliary variable defined in (12)	III.B
Θ	Random variable which takes values of θ	II.B
σ_θ	Standard deviation of θ	III.B
μ_θ	Mean value of θ	III.B
Δ	Longitude (degrees) difference between M and ES	II.A
ϕ_{ES}	ES latitude (in degrees)	II.A
A_{Atm}	Atmospheric attenuation	II.B
A_T	Total attenuation of the link	II.B
$A_T(\theta)$	Total attenuation of the link as a function of θ	III.B
$E[\cdot]$	Expected value operator	III.C
f_Θ	Probability density function of the elevation angle	III.A
F_Θ	Cumulative distribution function of the elevation angle	III.A
G_R	Receiver antenna gain	II.B
G_T	Transmitter antenna gain	II.B
G/T	Figure of merit (in this case, for the ES receiver system)	II.B
L_{FS}	Free space path loss	II.B
M	Subsatellite point (Instantaneous latitude and longitude of the satellite)	II.A
nQ	n -Quartile, $n \in \{1, 2, 3\}$	III.C
p_e	Exceedance probability for the attenuation model, also expressed as percentage	III.B
P_{out}	Outage probability	II.B
P_R	Received power	II.B
P_{Req}	Required received power	II.B
P_{th}	Threshold value for P_R	II.B
$r_{E,O}$	distance from the center of the Earth to the ES	II.A
$r_{S,O}$	distance from the center of the Earth to the satellite	II.A
$r_{S,E}$	distance from the ES to the satellite	II.B

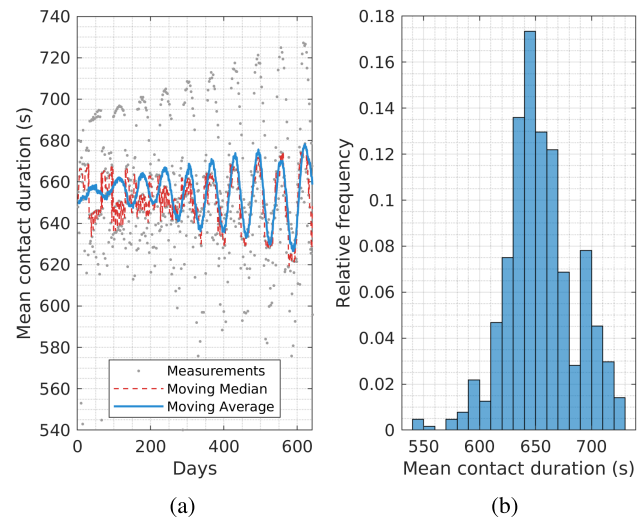
TABLE 2. Simulation parameters.

Simulation period	640 days (1.75 years)
ES location	25.6566°N, 100.2879°W
orbit eccentricity (e)	0
orbit inclination (i)	40°
semi-major axis (a)	7351 km

Fig. 2(a) shows the mean contact duration per day using gray dots, its moving average in blue, and the moving median in red, using a window size of 30 contacts, which corresponds to approximately five days. Orbital perturbations [24], that are not emphasized in this article, cause the oscillations. Those oscillations are small compared to the values shown in the moving average and median in the 640 days of the simulation. In the last days of the simulation, the moving average and median are just about 30s longer than those in the initial days; this is a good indicator, showing that the satellite behavior is very similar during the simulation period. Fig. 2(b) contains the histogram of the daily mean contact duration, showing that the values around 650s have the highest relative frequencies.

A. CHARACTERIZATION OF θ AS A RANDOM VARIABLE

From the values of θ obtained through the simulation, its probability density function (PDF), f_Θ , and cumulative distribution function (CDF), F_Θ , were fitted with those of the

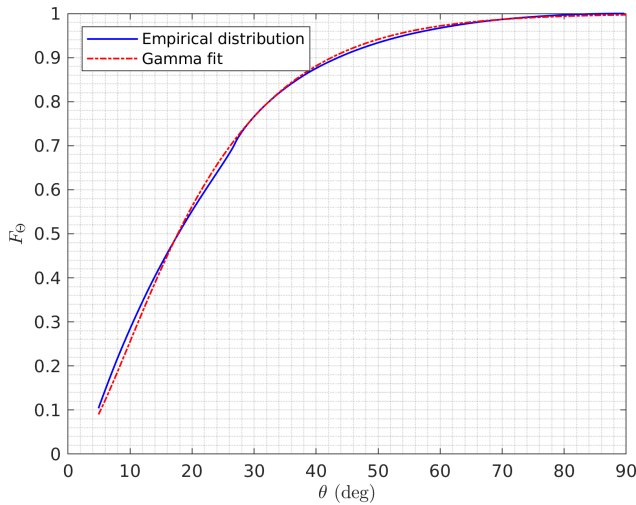
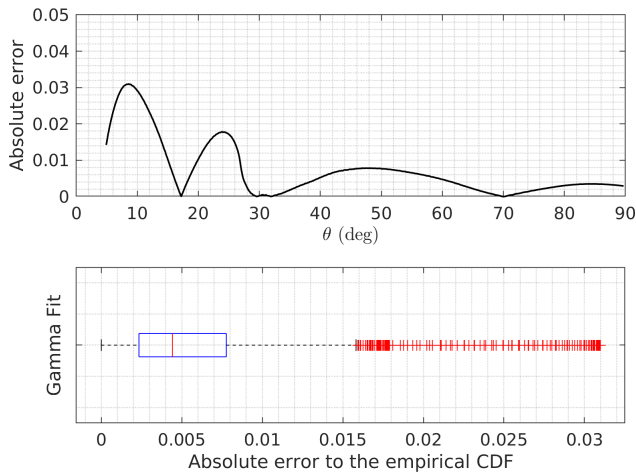
**FIGURE 2.** Values of the daily mean contact duration for circular LEO orbit using (a) data points, and (b) histogram.

gamma distribution, which are respectively given by

$$f_\Theta = \frac{1}{b^a \Gamma(a)} \theta^{a-1} \exp(-\theta/b), \quad (9)$$

and

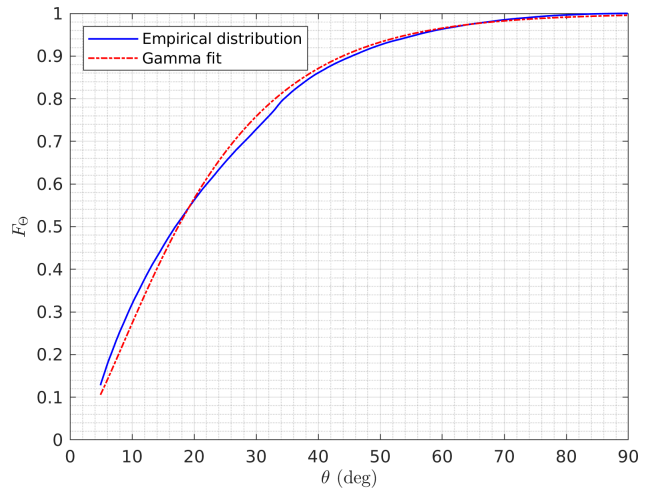
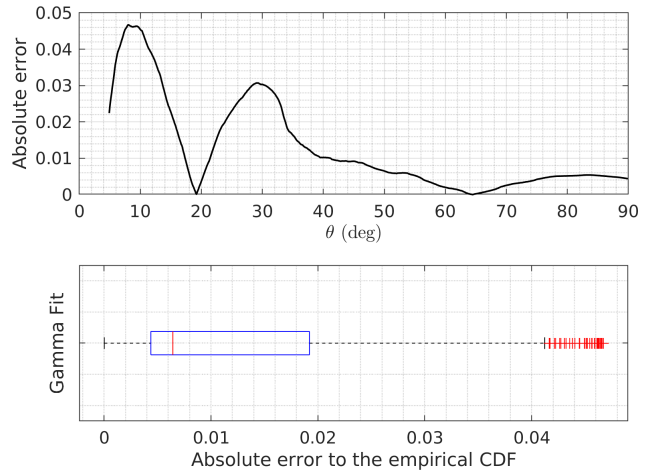
$$F_\Theta = \frac{1}{\Gamma(a)} \gamma \left(a, \frac{\theta}{b} \right), \quad (10)$$

FIGURE 3. Empirical vs Gamma CDF for $a = 7751$ km and $i = 50^\circ$.FIGURE 4. Gamma CDF vs Empirical CDF absolute error plots, for $a = 7751$ km and $i = 50^\circ$.

where a is the shape and b is the scale parameter, and $\gamma(\cdot)$ is the incomplete gamma function.

The parameters for the PDF f_θ were obtained using the maximum likelihood estimation method, and the CDF of θ was compared against its kernel distribution using the quadratic error. However, an analytical approach to characterize f_θ is available in [25] to obtain both f_θ and F_θ instead of simulation results or ephemeris files.

More simulations were performed extensively for different ES locations, orbit inclinations, and altitudes, showing also good fit to the Gamma distribution. Fig. 3 and Fig. 5 show the Gamma fit for F_θ for two ES's located at different latitudes, and for satellites with different orbit configurations as shown in Table 3, whereas Fig. 4 and Fig. 6 show their corresponding error plots. As mentioned before at the beginning of Section III, three remaining orbital parameters not included in Table 3 are set as $\omega = 0$, $\Omega = 0$, and $v = 0$. Fig. 4 and Fig. 6 show two kinds of error plots, the first indicates the absolute

FIGURE 5. Empirical vs Gamma CDF for $a = 8151$ km and $i = 80^\circ$.FIGURE 6. Gamma CDF vs Empirical CDF absolute error plots, for $a = 8151$ km and $i = 80^\circ$.

error between the empirical F_θ and the calculated Gamma CDF; and the second plot contains a boxplot of the absolute error, showing that the errors are less than 5% for at least the first three quartiles (which corresponds to 75% of the errors). The performed simulations and analysis show the suitability of using the gamma distribution to characterize the elevation angle for more ES locations and orbit configurations.

Also, it is possible to calculate the probability of contacts above a value of θ , e.g., θ_{min} , using the complementary function of (10) as follows

$$\bar{F}_\theta = P(\Theta \geq \theta) = 1 - F_\theta, \quad (11)$$

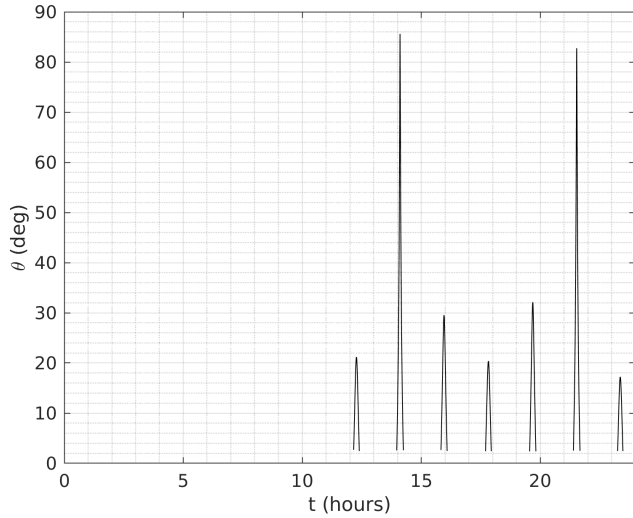
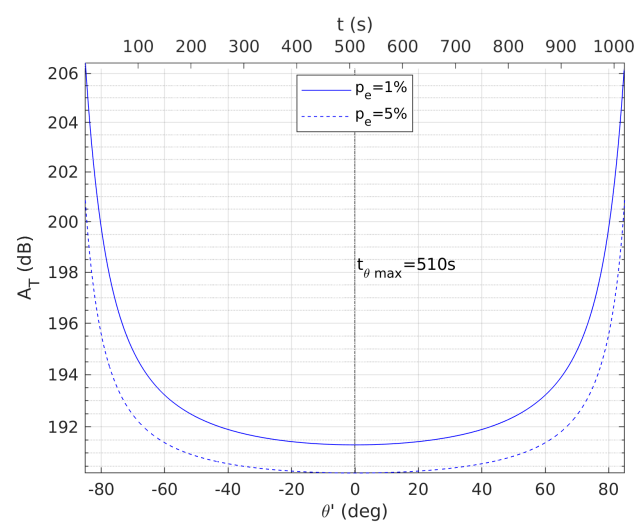
which in addition to (10), can be applied to calculate the quantiles of θ and P_R as will be shown in IV-B2.

B. CHARACTERIZATION OF A_T AS A FUNCTION OF θ

Once f_θ and F_θ were obtained, we calculate A_{Atm} as described by ITU-R P.618-13, [26], considering rain, gas, clouds, and fog attenuation; then, L_{FS} was added to obtain A_T . Finally,

TABLE 3. Gamma distribution fit for the elevation angle PDF and CDF with other orbit configuration and ES locations.

Semi-major axis, a	Orbit inclination, i	Orbit eccentricity, e	ES location	Shape parameter for f_Θ	Scale parameter parameter for f_Θ
7751 km	50	0	35°N, 100.2879°W	1.8408	11.6368
8151 km	80	0	65°N, 100.2879°W	1.6530	13.0686

**FIGURE 7.** Contacts for one simulation day.**FIGURE 8.** Total attenuation for a contact with $f_c = 20$ GHz and $\theta \approx 90^\circ$.

the transmitter EIRP and G_R where coherently added in logarithmic units in the link budget as in (8).

The calculated A_{Atm} values come from a well known approach that can be developed also for other locations using the data sets already provided with the ITU Recommendations, or other available local data. However, there are more attenuation models in the literature to characterize A_{Atm} , such as probabilistic models [27] that assume correlation between the atmospheric losses. Nevertheless, all of those models need to be adapted to the variable elevation angle conditions produced by LEO.

A LEO satellite is visible for short periods of time as shown in Fig. 7, which contains all the contacts (in a 24-hour format) for one of the simulation days, and where it is observable the variability of θ and θ_{max} . Each time the satellite appears over the horizon, θ is at its lowest value and increases until it reaches its maximum point, θ_{max} , to decrease again. For each contact, θ_{max} coincides with the minimum A_T . Fig. 8 shows A_T for a contact with $\theta_{max} \approx 90^\circ$, and it includes for simplicity an auxiliary variable (θ') defined as follows

$$\theta' = \begin{cases} \theta - 90 \text{ deg} & \text{for } t \leq t_{\theta_{max}} \\ 90 - \theta \text{ deg}, & \text{for } t > t_{\theta_{max}} \end{cases} \quad (12)$$

As it can be observed in Fig. 8, A_T is symmetrical with respect to the time at which θ_{max} occurs, $t_{\theta_{max}}$, and it is the same for equal values of θ ; then, A_T can be approximated by a polynomial function of θ , $A_T(\theta)$, using the A_T data of a

contact with $\theta_{max} \approx 90^\circ$ as follows

$$A_T(\theta) = \sum_{k=0}^K a_k \left(\frac{\theta - \mu_\theta}{\sigma_\theta} \right)^{K-k}, \quad (13)$$

where $A_T(\theta)$ is in dB, a_k are the polynomial coefficients, and μ_θ and σ_θ are the mean and standard deviation, respectively, of the θ values corresponding to the $A_T(\theta)$ data. Different A_T curves can be calculated for several attenuation scenarios such as multiple rainfall rates, or different values of exceedance probability, p_e , of the total attenuation. The A_T data representation, that we propose through (13) is just one of the available options to characterize the A_T data as a function of θ . One can also select other methods such as spline curves, lookup tables, as well as interpolation.

C. PROPOSED LINK BUDGET

Typical LEO link budget analysis involves the calculation of the received power at the shortest and largest link paths. The maximum link length occurs at the minimum elevation angle, θ_{min} , which satisfies a received power threshold, P_{th} . Nevertheless, θ_{min} , which is preferably located close to the local horizon, should be chosen large enough to skip any significant local obstructions (e.g., θ_{min} satisfies P_{th} and is large enough to skip tall buildings or mountains). On the other hand, the minimum link length occurs close to the maximum elevation angle, θ_{max} , which ideally coincides with the ES zenith, and with the minimum value of $r_{S,E}$.

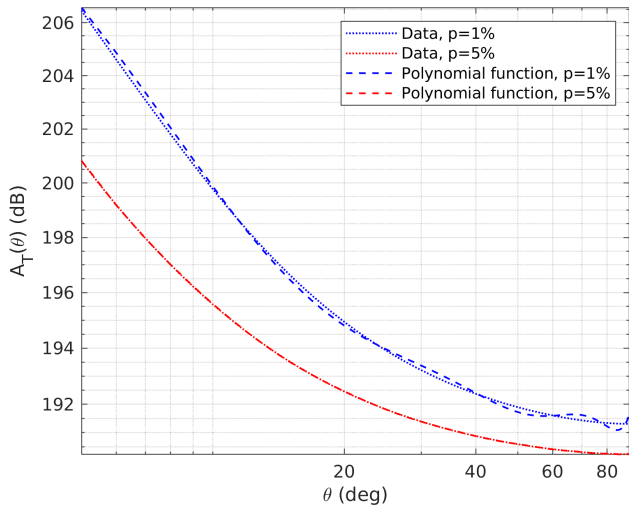


FIGURE 9. $A_T(\theta)$ and its polynomial representation.

With obstructed line of sight conditions, the best and worst-case elevation angle for a particular ES location can be determined by several methods, including geometrical-based approximations using data of the obstacles height and position as in [28]. Another approach based on digital hemispherical photographs has been utilized by [29] and more recently, by [30] and [31], among others, to extract the elevation angle conditions of a particular location. This approach based on hemispherical images is an easy-to-implement methodology (e.g., compared to terrestrial laser scanning [32]) that can provide detailed information about the elevation angle and the ES environment.

Knowing the transmitter EIRP and G_R , one can calculate the values of θ_{min} and $A_T(\theta_{min})$ from the polynomial approximation $A_T(\theta)$ as well as the attenuation at θ_{max} to have the best and worst cases of (8). However, the value of θ_{min} should be verified to be non-obstructed (above any obstruction), and in case the calculated value of θ_{min} is not suitable, it could be replaced by a larger value above enough local obstructions as mentioned at the beginning of this subsection.

After determining a value for θ_{min} , to develop the proposed link budget, first, we calculate the expected received power, $E[P_R]$, with the assumptions in (3)-(7) which consider constant transmitted power and receiver antenna gain, as well as A_T dependent only on the distance and atmospheric conditions.

The expected value of the received power can be calculated from (8), and using $A_T(\theta)$ as defined in (13) as follows

$$\begin{aligned} E[P_R] &= E[\text{EIRP} + G_R + A_T(\theta)] \\ &= \text{EIRP} + G_R + A_T(E[\theta]), \end{aligned} \quad (14)$$

or it can be further worked to describe P_R for a desired range of θ , e.g., the region outside outage, that is

$$E[P_R|\theta \geq \theta_{min}] = \text{EIRP} + G_R + A_T(E[\theta|\theta \geq \theta_{min}]), \quad (15)$$

where

$$E[\theta|\theta \geq \theta_{min}] = \int_{\theta_{min}}^{\theta_{max}} \theta f_{\Theta}(\theta|\theta \geq \theta_{min}) d\theta, \quad (16)$$

and for simplicity it can be rewritten as in [33] as

$$E[\theta|\theta \geq \theta_{min}] = \frac{\int_{\theta_{min}}^{\theta_{max}} \theta f_{\Theta}(\theta) d\theta}{F_{\Theta}(\theta_{max}) - F_{\Theta}(\theta_{min})}, \quad (17)$$

The numerical value of the variance and standard deviation of the received power can be obtained from the variance of θ , which we get as follows

$$\begin{aligned} \text{Var}[\theta|\theta \geq \theta_{min}] &= E[\theta^2|\theta \geq \theta_{min}] \\ &\quad - E[\theta|\theta \geq \theta_{min}]^2, \end{aligned} \quad (18)$$

The standard deviation of the received power can be calculated from an interval of the received power caused by one standard deviation of θ such as

$$\text{SD}[p_R] = p_R(E[\theta] + \text{SD}[\theta]) - p_R(E[\theta]), \quad (19)$$

where p_R is the received power in linear units, and $\text{SD}[\theta]$ or $\text{SD}[\theta|\theta > \theta_{min}]$ are obtainable from (18).

Then, the link budget can be expressed with its expected receiver power, variance, and standard deviation, in addition to the common best and worst cases. Additionally, the quartiles ($nQ: n \in \{1, 2, 3\}$) can be obtained through the inverse CDF (ICDF) of θ , which can be evaluated numerically for the gamma distribution. The link margin can also be evaluated as the difference between P_{Req} and any of the link indicators such as $E[P_R]$.

Fig. 10(a) shows the trajectory of a satellite going from position S_1 to S_3 , with its corresponding link distances $r_{S_1,E}$, $r_{S_2,E}$, and $r_{S_3,E}$. Even though $r_{S,O}$ is constant for a circular orbit, $r_{S,E}$ is not, and it will be larger when the spacecraft is close to the horizon. Fig. 10(b) shows the largest link length (which occurs at θ_{min}), which is the worst case scenario, because it has the greatest value of A_T as discussed in Section II. Similarly, the best-case occurs at the shortest link path (ideally at $\theta = 90^\circ$). LEO link budgets commonly analyze the received power only for the best and worst-cases. However, this description can be enhanced considering not only the extreme ranges (best and worst-cases), but also including the set of all possible values of the elevation angle to obtain relevant quantities as proposed in this section and shown in Fig. 10(c).

Although it is not further discussed in this article, statistics of the received power such as its minimum, expected value, and quantiles, can be individually obtained for satellites in diverse orbits of a constellation with the same methodology proposed here. Additionally, the link margins and P_R statistics can be helpful in the estimation of required handovers since those usually depend on the variable distance to the satellite (which is implicitly addressed in this article by considering the elevation angle variability), or on performance indicators such as C/N (which can be easily obtained from P_R as mentioned in Section II-C). However, handovers for LEO satellites depend on more factors, such as traffic load, which are discussed in works such as [34] and [35].

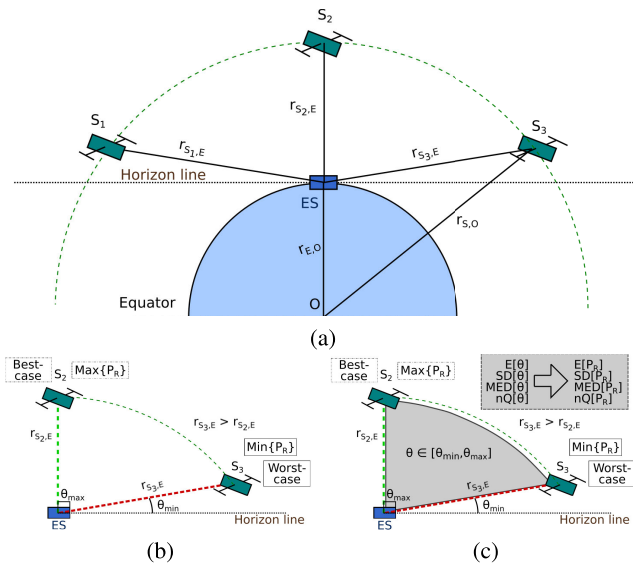


FIGURE 10. Considerations for the proposed link budget.

TABLE 4. Coefficients for the polynomial approximation of A_T .

Parameter	$p_e=1.00\%$	$p_e=5.00\%$
a_0	0.430	0.463
a_1	-2.091	-2.153
a_2	2.891	2.578
a_3	-0.636	-0.331
a_4	0.277	-0.700
a_5	-2.427	-1.616
a_6	193.140	191.449
μ_θ	32.329	
σ_θ	24.203	

IV. RESULTS

This section presents numerical results for a common LEO link budget using θ_{min} and θ_{max} for its calculation; and the proposed link budget, based on f_Θ and its statistics. The two link budget calculations use the polynomial approximation of $A_T(\theta)$ which was first introduced in Section III-B.

A. CHARACTERIZATION OF A_T

In this section we present the characterization of A_T as a function of θ as it was explained in Section III-B. Table 4 contains the polynomial coefficients for two curves of A_T for $p_e = 1.00\%$ and $p_e = 5.00\%$, for the ES location shown in Table 2. The polynomial coefficients were obtained from the numerical data of Fig. 8 using (13), the number of coefficients is the minimum to satisfy a maximum error criterion (arbitrarily chosen) of 0.5 dB for $A_T(\theta)$. Fig. 9 shows the calculated values of $A_T(\theta)$ and its polynomial representation obtained thought coefficients of Table 4.

B. LINK BUDGET CALCULATIONS

Here we present the calculations for the link budget. First introducing the results of a typical LEO link budget and then, presenting the results for the proposed link budget as explained in Section III-C.

TABLE 5. Best and worst case of link budget.

	Worst case		Best case	
Exceedance	1.00%	5.00%	1.00%	5.00%
θ (deg)	9	5	90	90
$A_T(\theta)$ (dBi)	201	201	191.4	190.6
EIRP (dBW)			56	
G_R (dBi)			40	
P_R (dBW)	-105	-105	-95.4	-94.6
P_{Req} (dBW)			-105	
Margin (dB)	0	0	9.6	10.4

TABLE 6. Parameters for the distributions of θ and θ_{max} .

Parameters for f_Θ and F_Θ
$a = 1.79$
$b = 10.43$

1) TYPICAL LINK BUDGET FOR LEO

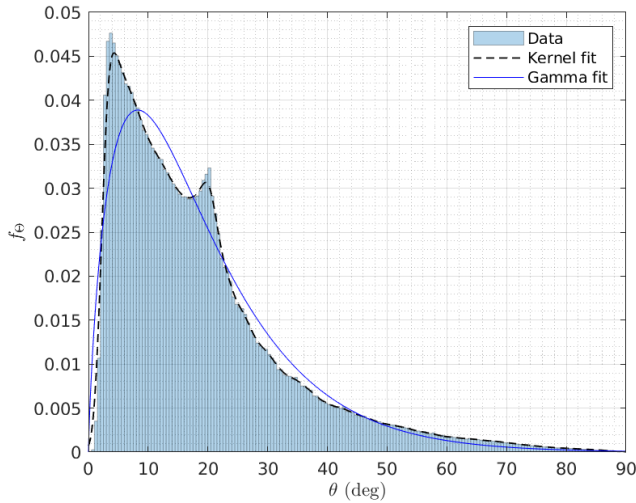
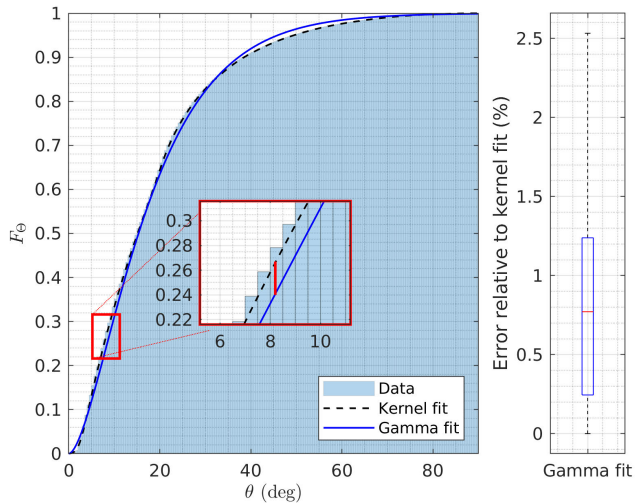
A link budget calculation was developed for a satellite with the orbit characteristics of Table 2, a transmitter EIRP of 56 dBW, G_R of 40 dBi, and a carrier frequency, f_c , of 20 GHz. The required received power, P_{Req} , is -105 dBW, then from (8), the maximum allowable value of A_T for satisfying this requirement is 201 dBi. From those specifications, a classical link budget analysis can be developed as shown in Table 5.

For the link budget best-case, where the satellite is closest to the ES, the value of θ that satisfies the received power requirement is $\theta_{min} = 5^\circ$ for $p_e = 1\%$ and $\theta_{min} = 9^\circ$ for $p_e = 5\%$. The value of θ_{max} is assumed to be 90° , that is, when the satellite is just above the ES. The worst case value of θ , θ_{min} , is calculated from the polynomial of (13) and the P_R requirement, P_{Req} , as $A_T(\theta_{min}) = -201$ dB; however, in the case of considerable obstructions, it could be replaced by a larger value as mentioned in Section III-C.

2) PROPOSED LINK BUDGET FOR LEO

For the proposed link budget, the distribution parameters of (9)-(10) were first obtained from the recorded values of θ as shown in Table 6. Fig. 11 shows the histogram of Θ , and its PDF approximated by both a kernel distribution and by (9). Similarly, Fig. 12 shows the CDF's of Θ , and a box plot indicating the absolute error between the kernel and gamma distributions. The maximum error value was about 2.5%, or about 0.025 for F_Θ , as shown in the region inside the red box in the CDF graph; but, for 75% of the data it was below 1.25%.

Since the mean and expected value of P_R depend on θ , it is convenient to first obtain its statistics. Table 7 contains the required statistical information of θ obtained from its recorded values, in the columns labeled as data; as well as from analysis and use of the properties of the gamma distribution, in the columns labeled as gamma. Those statistics are obtained for the same p_e and θ_{min} values as those used for the link budget calculations of Table 5.

FIGURE 11. PDF of θ .FIGURE 12. CDF of θ .TABLE 7. Statistics of θ in deg.

	Gamma	9°	Gamma	Data
θ_{min}				
θ_{max}	90	89.89	90	89.89
$E[\theta]$	25.64	24.28	21.20	21.00
$1Q[\theta]$	13.94	14.22	10.77	10.46
$MED[\theta]$	20.06	20.14	17.27	17.42
$3Q[\theta]$	29.56	29.65	27.03	26.48
$VAR[\theta]$	88.75	197.04	167.44	206.11
$SD[\theta]$	9.42	14.03	12.94	14.36

From the results of Table 7, $A_T(\theta)$ is evaluated in Table 8 according to (13) with the coefficients of Table 4. The values of $A_T(\theta)$ obtained from the statistics of the analytical function f_θ are in the columns labeled as gamma. The actual $A_T(\theta)$ values are in the columns labeled as data.

Finally, Table 9 shows the link budget including the calculated values for $E[P_R|\theta \geq \theta_{min}]$, $SD[P_R|\theta \geq \theta_{min}]$, and the quartiles $nQ[P_R|\theta \geq \theta_{min}]$, for the same values of θ_{min}

TABLE 8. Statistics of A_T in dB's.

	Gamma	Data	Gamma	Data
θ_{min}	9°			5°
θ_{max}	90°	89.89°	90°	89.89°
$\text{Min}\{A_T(\theta)\}$	191.65	191.31	190.64	190.24
$\text{Max}\{A_T(\theta)\}$	200.89	200.72	201.01	200.82
$E[A_T(\theta)]$	193.87	194.03	192.18	192.31
$1Q[A_T(\theta)]$	197.00	196.99	195.16	195.32
$\text{MED}[A_T(\theta)]$	194.79	194.91	192.72	192.93
$3Q[A_T(\theta)]$	193.42	193.25	191.77	191.66
$A_T(E[\theta] + SD[\theta])$	192.87	192.48	191.32	191.08

TABLE 9. Link budget in dBW considering θ as a random variable.

	Gamma	Data	Gamma	Data
Exceedance	1%		5%	
θ_{min}	9°		5°	
EIRP	56 dBW		56 dBW	
G_R	40 dBi		40 dBi	
$\text{Min}\{P_R \theta \geq \theta_{min}\}$	-104.89	-104.72	-105	-105
$\text{Max}\{P_R \theta \geq \theta_{min}\}$	-95.65	-95.31	-94.64	-94.61
$E[P_R \theta \geq \theta_{min}]$	-97.87	-98.03	-96.17	-96.19
$1Q[P_R \theta \geq \theta_{min}]$	-101.00	-100.99	-99.16	-99.36
$\text{MED}[P_R \theta \geq \theta_{min}]$	-98.79	-98.91	-96.72	-96.80
$3Q[P_R \theta \geq \theta_{min}]$	-97.42	-97.25	-95.77	-94.61
$SD[P_R \theta \geq \theta_{min}]$	42.28pW	67.51pW	52.77pW	76.57pW

as those used for the link budget in Table 5. The margin of P_R can be expressed as the difference between the required power and any of the indicators of P_R such as its expected value, or median as

$$\text{Link margin} = E[P_R] - (P_R)_{REQ}. \quad (20)$$

V. CONCLUSION AND FUTURE WORK

This work presented a methodology to evaluate a LEO satellite link considering the ever-changing elevation angle, θ . The variability of θ was characterized through a gamma distribution, showing a good description of the actual behavior. Using the obtained PDF and CDF of θ , the statistics of P_R such as the expected received power were later calculated. Additionally, the quantiles of P_R allowed the quantification of the probability of P_R being above or below certain threshold level.

The characterization of the elevation angle through a random variable can be expanded for more ES locations and orbit configurations as mentioned in Section III-A. The gamma distribution offered a good fit of the actual θ behavior, specially for the CDF, and simplified the process to calculate the statistics of the elevation angle. The maximum observed absolute error between the empirical and gamma CDF for θ was around 0.05 (5%), but the error was much below 5% for more than 75% of all the points in the CDF.

Differences between the empirical PDF of the elevation angle and the gamma PDF were observed in Fig. 11. However, the gamma distribution was able to represent the behavior of the elevation angle in the CDF as shown in Fig. 12. The small errors between the empirical CDF and gamma CDF show that the gamma distribution is a suitable alternative to characterize the elevation angle behavior for different ES locations and orbit configurations.

In addition to the statistical characterization of θ , the proposed link budget analysis develops not just the best and worst cases of the received power as it is commonly done in typical link budgets for LEO satellite, but restricts those cases to the minimum and maximum values of P_R , and provides additional statistical descriptors as the expected value for P_R , its standard deviation, median, and quartiles.

Finally, even though the link analysis was developed for a particular ES location, the developed methodology can be applied to more ES's at diverse locations as it was shown in Section III, and with different link characteristics (e.g., EIRP or antennas gain). Also, the methodology can be extended to the uplink by replacing the downlink parameters. Furthermore, the values of P_R can be utilized to calculate related link indicators, such as C/N and C/N_0 , by considering the particular characteristics of the receiver and transmitter system, such as the figure of merit, G/T .

REFERENCES

- [1] I. D. Portillo, B. G. Cameron, and E. F. Crawley, "A technical comparison of three low earth orbit satellite constellation systems to provide global broadband," *Acta Astronautica*, vol. 159, pp. 123–135, Jun. 2019.
- [2] G. E. Corazza and F. Vatalaro, "A statistical model for land mobile satellite channels and its application to nongeostationary orbit systems," *IEEE Trans. Veh. Technol.*, vol. 43, no. 3, pp. 738–742, Aug. 1994.
- [3] C. Kourogiorgas, M. Kvicera, and D. Skraparlis, "Modeling of first-order statistics of the MIMO dual polarized channel at 2 GHz for land mobile satellite systems under tree shadowing," *IEEE Trans. Antennas Propag.*, vol. 62, no. 10, pp. 5410–5415, Oct. 2014.
- [4] International Telecommunication Union, *ITU Handbook on Satellite Communications*. 3rd ed. Hoboken, NJ, USA: Wiley, 2002.
- [5] G. Maral, M. Bousquet, and Z. Sun, *Satellite Communications Systems*. 6th ed. Hoboken, NJ, USA: Wiley, 2020.
- [6] S. Cornara, T. W. Beech, M. Belló-Mora, and G. Janin, "Satellite constellation mission analysis and design," *Acta Astronautica*, vol. 48, nos. 5–12, pp. 681–691, Mar. 2001.
- [7] G. Buttazzoni, M. Comisso, A. Cuttin, M. Fragiocomo, R. Vescovo, and R. V. Gatti, "Reconfigurable phased antenna array for extending cubesat operations to Ka-band: Design and feasibility," *Acta Astronautica*, vol. 137, pp. 114–121, Aug. 2017.
- [8] P. Marzilli, L. Gugliermetti, F. Santoni, A. Delfini, F. Piergentili, L. Nardi, G. Metelli, E. Benvenuto, S. Massa, and E. Bennici, "CultCube: Experiments in autonomous in-orbit cultivation on-board a 12-units CubeSat platform," *Life Sci. Space Res.*, vol. 25, pp. 42–52, May 2020.
- [9] S. Pätzschke and S. Klinkner, "Towards a highly adaptive software-defined radio transmitter for small satellite platforms," *Acta Astronautica*, vol. 186, pp. 50–59, Sep. 2021.
- [10] COST 255, *Radiowave Propagation Modelling for New Satcom Services at Ku-Band and Above*, ESA Publications Division, document SP-1252, 2002.
- [11] A. Nandra, J. Govil, and H. Kaur, "Optimization of satellite link design," in *Proc. IEEE SoutheastCon*, Huntsville, AL, USA, Apr. 2008, pp. 147–152.
- [12] S. C. Ekpo, "Parametric system engineering analysis of capability-based small satellite missions," *IEEE Syst. J.*, vol. 13, no. 3, pp. 3546–3555, Sep. 2019.
- [13] U. Lewark, J. Antes, J. Walheim, J. Timmermann, T. Zwick, and I. Kallfass, "Link budget analysis for future E-band gigabit satellite communication links (71–76 and 81–84 Ghz)," *CEAS Space J.*, vol. 4, nos. 1–4, pp. 41–46, 2013.
- [14] Y. Seyedi and F. Rahimi, "A trace-time framework for prediction of elevation angle over land mobile LEO satellites networks," *Wireless Pers. Commun.*, vol. 62, no. 4, pp. 793–804, Feb. 2012.
- [15] A. Babuscia, B. Corbin, R. Jensen-Clem, M. Knapp, I. Sergeev, M. Van de Loos, and S. Seager, "CommCube 1 and 2: A cubesat series of missions to enhance communication capabilities for cubesat," in *Proc. IEEE Aerosp. Conf.*, Mar. 2013, pp. 1–19.
- [16] D. Barbaric, J. Vukovic, and D. Babic, "Link budget analysis for a proposed cubesat Earth observation mission," in *Proc. 41st Int. Conv. Inf. Commun. Technol., Electron. Microelectron. (MIPRO)*, May 2018, pp. 133–138.
- [17] I. Latachi, M. Karim, A. Hanafi, T. Rachidi, A. Khalayoun, N. Assem, S. Dahbi, and S. Zouggar, "Link budget analysis for a LEO cubesat communication subsystem," in *Proc. Int. Conf. Adv. Technol. Signal Image Process. (AT SIP)*, May 2017, pp. 1–6.
- [18] O. Popescu, "Power budgets for cubesat radios to support ground communications and inter-satellite links," *IEEE Access*, vol. 5, pp. 12618–12625, 2017.
- [19] M. O. Kolawole, *Satellite Communication Engineering*. New York, NY, USA: Marcel Dekker, 2002.
- [20] P. Arapoglou and A. D. Panagopoulos, "A tool for synthesizing rain attenuation time series in LEO Earth observation satellite downlinks at Ka band," in *Proc. 5th Eur. Conf. Antennas Propag. (EUCAP)*, Apr. 2011, pp. 1467–1470.
- [21] S. K. Sharma, S. Chatzinotas, and B. Ottersten, "In-line interference mitigation techniques for spectral coexistence of GEO and NGEO satellites," *Int. J. Satell. Commun. Netw.*, vol. 34, no. 1, pp. 11–39, 2014.
- [22] C. Wang, D. Bian, S. Shi, J. Xu, and G. Zhang, "A novel cognitive satellite network with GEO and LEO broadband systems in the downlink case," *IEEE Access*, vol. 6, pp. 25987–26000, 2018.
- [23] Y. Su, Y. Liu, Y. Zhou, J. Yuan, H. Cao, and J. Shi, "Broadband LEO satellite communications: Architectures and key technologies," *IEEE Wireless Commun.*, vol. 26, no. 2, pp. 55–61, Apr. 2019.
- [24] V. A. Chobotov, *Orbital Mechanics*, 3rd ed. Reston, VA, USA: AIAA Press, 2002.
- [25] S.-Y. Li and C. H. Liu, "An analytical model to predict the probability density function of elevation angles for LEO satellite systems," *IEEE Commun. Lett.*, vol. 6, no. 4, pp. 138–140, Apr. 2002.
- [26] *Propagation Data and Prediction Methods Required for the Design of Earth-Space Telecommunication Systems*, Recommendation, document ITU-R P.618-13, 2017.
- [27] A. G. Kanatas and A. D. Panagopoulos, *Radio Wave Propagation and Channel Modeling for Earth-Space Systems*. Boca Raton, FL, USA: CRC Press, 2015.
- [28] H. H. Moghadam and A. B. Kouki, "New modified urban canyon models for satellite signal propagation prediction," *IEEE Access*, vol. 7, pp. 25298–25307, 2019.
- [29] J. E. Colcord, "Using fish-eye lens for GPS site reconnaissance," *J. Surveying Eng.*, vol. 115, pp. 347–352, Aug. 1989.
- [30] M. Rieche, A. Ihlow, D. Arndt, F. Pérez-Fontán, and G. Del Galdo, "Modeling of the land mobile satellite channel considering the terminal's driving direction," *Sensors*, vol. 2015, Mar. 2015, Art. no. 372124.
- [31] M. J. L. Lee, S. Lee, H.-F. Ng, and L.-T. Hsu, "Skymask matching aided positioning using sky-pointing fisheye camera and 3D city models in urban canyons," *Int. J. Antennas Propag.*, vol. 20, no. 17, p. 4728, Aug. 2020.
- [32] R. Pelc-Mieczkowska, "Comparison of selected data acquisition methods for GNSS terrain obstacles modeling," *Acta Geodynamica et Geomaterialia*, vol. 12, no. 3, pp. 307–315, Jul. 2015.
- [33] A. Papoulis, *Probability, Random Variables, and Stochastic Processes*, 2nd ed. New York, NY, USA: McGraw-Hill, 1984.
- [34] T. Leng, Y. Xu, G. Cui, and W. Wang, "Caching-aware intelligent handover strategy for LEO satellite networks," *Remote Sens.*, vol. 13, no. 11, p. 2230, Jun. 2021.
- [35] Y. Liu, L. Feng, L. Wu, Z. Zhang, J. Dang, B. Zhu, and L. Wang, "Joint optimization based satellite handover strategy for low Earth orbit satellite networks," *IET Commun.*, vol. 15, pp. 1576–1585, Mar. 2021.



JUAN MISAELO GONGORA-TORRES (Graduate Student Member, IEEE) received the B.Sc. degree in mechatronics and the M.Sc. degree in telecommunications from the Tecnológico de Monterrey, where he is currently pursuing the Ph.D. degree with the Department of Telecommunications and Networks. His research interests include outdoor channel characterization, space communications, satellite communications, and signal processing. He is also an IEEE-HKN Lambda-Rho Chapter Inducted Member and the current President.



CESAR VARGAS-ROSALES (Senior Member, IEEE) received the M.Sc. and Ph.D. degrees in communications and signal processing and electrical engineering from Louisiana State University. He is the coauthor of the books *Position Location Techniques and Applications* (Academic Press/Elsevier) and *Radio Wave Propagation in Vehicular Environments* (IET). His research interests include personal communications, 5G/6G, cognitive radio, MIMO systems, stochastic modeling, interference, intrusion/anomaly detection, position location, satellite communications, and error correcting codes. He is a member of the Mexican National Researchers System (SNI), the Mexican Academy of Science (AMC), and the Academy of Engineering of Mexico (AIM). He is a Senior Member of the IEEE Communications Society and was the Monterrey Chapter Chair. He has also been the Faculty Advisor of the IEEE-HKN Lambda-Rho Chapter with Tecnológico de Monterrey. He was also the Technical Program Chair of the IEEE Wireless Communications and Networking Conference (IEEE WCNC). He serves as an Associate Editor for IEEE ACCESS and the *International Journal of Distributed Sensor Networks*, and a Guest Editor of the *Applied Sciences* journal.



ALEJANDRO ARAGÓN-ZAVALA (Senior Member, IEEE) received the B.Sc. degree in electronics and communications engineering from the Tecnológico de Monterrey, Querétaro, Mexico, in 1992, the M.Sc. degree in satellite communication engineering from the University of Surrey, U.K., in 1997, and the Ph.D. degree in antennas and propagation from the Centre for Communication System Research, University of Surrey, in 2003. He worked as a Senior In-Building Radio Consultant with Cellular Design Services Ltd., U.K., from 1998 to 2003,

and the Program Chair of the B.Sc. degree with Electronics Engineering Program, from 2003 to 2008, the Head of the Mechatronics Department, from 2008 to 2011, and the Head of the Computing Regional Department, from 2019 to 2020, all with the Tecnológico de Monterrey, where he is currently a Titular Professor with the School of Engineering and Science, Tecnológico de Monterrey, and a Wireless Expert Senior Associate Consultant with Real Wireless Ltd., U.K. He is the author of more than 40 research articles, three electronic books, and three printed books on wireless communications aspects. His research interests include indoor radio propagation, high-altitude platforms (HAPS), industry 4.0, vehicular technologies, satellite communications/engineering, broadcasting, and channel modeling.



RAFAELA VILLALPANDO-HERNANDEZ received the M.Sc. degree in electronic engineering (telecommunications) and the Ph.D. degree in communications and information technologies from the Instituto Tecnológico y de Estudios Superiores de Monterrey (ITESM), Monterrey, in December 2008. She joined the Engineering Center, ITESM, Laguna, Torreon, Mexico. She has participated in several research projects involving network coding, security algorithms, position location in wireless networks, and implementation of sensor networks. Her research interest includes wireless and sensor networks. She is a member of the Mexican National Researchers System (SNI) Level I.

• • •